Structural Aspects and Orientation Mechanism of Mitochondrial F_1 Adenosinetriphosphatase. Evidence for a Negative Electric Birefringence due to a Permanent Moment Perpendicular to the Long Axes of the Particle†

Gilbert Deléage, Bernard Roux, and Christian Marion*

Laboratoire de Physico-Chimie Biologique, LBTM-CNRS UM 24, Université Claude Bernard, Lyon I, 69622 Villeurbanne Cédex, France

Received October 31, 1985; Revised Manuscript Received January 23, 1986

ABSTRACT: The electric birefringence technique was used to investigate the steady-state birefringence, the orientational relaxation time, and the orientation mechanism of pig heart mitochondrial F_1 adenosine-5′-triphosphatase (F_1-ATPase). The electrooptical properties of this enzyme in solution were studied as functions of pH, protein concentration, and applied electric field. The F_1-ATPase exhibits a surprising negative electric birefringence with a specific Kerr constant of -1.5×10^{-3} esu cgs. The field-independent relaxation time was found to be 0.65 ± 0.05 μs, corresponding to a rotational diffusion constant of 2.55×10^5 s^{-1}. The overall size and shape of F_1-ATPase have been calculated from both translational and rotational diffusion constants. The enzyme may be assumed to be an oblate ellipsoid of revolution with dimensions of about $170 \times 170 \times 70$ Å. The orientation mechanism of F_1-ATPase was analyzed by fitting experimental birefringence rising curves with theoretical rising functions. The ratio of the permanent to induced dipole moment is found to be very high; therefore, the birefringence of F_1-ATPase is due to a strong permanent dipole moment in a direction perpendicular to the long axes of the particle. These particular electric properties can be explained by the oligomeric structure of the protein and seem likely to play a role in its mechanism of functioning.

In energy-transducing membranes, the terminal enzyme of oxidative phosphorylation is the reversible adenosine-5′-triphosphatase (ATPase)[1]–ATP synthase complex (also called F_0F_1 complex) which catalyzes the synthesis of ATP from ADP and P_i. The F_0F_1 complex is reputed to behave as a proton pump (involving charge movement) since it utilizes a proton electrochemical gradient to synthesize ATP (Mitchell, 1961). This complex is composed of two sectors, a hydrophobic membrane embedded part (F_0) and a water-soluble part (F_1) extrinsic to the membrane. The F_0 part conducts protons across the membrane, and the F_1 part, which exhibits only ATP hydrolysis activity, contains the catalytic sites [for reviews, see Fillingame (1980), Amzel & Pedersen (1983), and Vignais & Satre (1984)]. The F_1 sector isolated from various sources consists of five different subunits, the stoichiometry of which is $\alpha_3\beta_3\gamma\delta\epsilon$. The molecular weight of this hydrophilic sector ranges from 300 000 to 400 000. Structural studies obtained by hydrodynamic methods (Wagner & Junge, 1982; Wagner et al., 1985) as well as X-ray (Süss et al., 1978; Paradies & Schmidt, 1979) and neutron scattering (Satre & Zaccai, 1979) and electron microscopy of single crystals (Ackey et al., 1983) led to the conclusion that F_1 is rather eccentric with an axial ratio of 1.5–2. F_1 has generally been described as an ellipsoid with a maximal dimension of 110–120 Å and a thickness of 70–80 Å. A detectable hollow cavity in the complex has been suggested (Satre & Zaccai, 1979; Amzel et al., 1982; Ackey et al., 1983).

Surprisingly, there is no available information on the electric properties of F_1-ATPase although they likely play an important role in its function.

We report here a study of size, shape, and orientation mechanism of pig heart mitochondrial F_1-ATPase by electric birefringence, a technique of considerable potential utility for addressing such questions [for reviews, see Fredericq & Houssier (1973), Yoshioka (1978), and Bernengo (1981)]. We have successfully used this sensitive method with its dual characteristics of rotational relaxation time and steady-state birefringence in the study of proteins (Roux & Cassoly, 1982) and nucleosomal structures (Marion & Roux, 1978; Marion, 1984) and to reveal fine conformational changes in chromatin fibers (Marion et al., 1985a,b). Since many functional properties of the F_0F_1 complex and of isolated F_1-ATPase have been studied in our laboratory (Godinot et al., 1975; Di Pietro et al., 1980; Deléage et al., 1983; Roux et al., 1984), the structural studies presented here using highly purified and well-characterized F_1-ATPase (Penin et al., 1979) may then contribute to a better knowledge of structure–function relationships in the F_0F_1 complex.

Materials and Methods

Biological Materials. Pig heart mitochondria were obtained as previously described (Godinot et al., 1969) and suspended in 0.25 M sucrose–10 mM Tris-HCl, pH 7.6. The mitochondrial F_1-ATPase was purified by the method of Penin et al. (1979). Finally, the obtained enzyme, highly active (Penin et al., 1979), was stored frozen at −70 °C in 100 mM Tris–H_2SO_4, 5 mM EDTA, and 50% glycerol, pH 8, at a concentration of 4.4 mg/mL. Just before electric birefringence measurements, the stock solution is incubated at 30 °C and diluted to obtain a final glycerol concentration of 20%. Purity was checked by SDS–15% polyacrylamide gel electrophoresis (Laemmli, 1970). The protein content of the enzyme solution

† This work was supported by the CNRS (UM 24).

[1] Abbreviations: ATPase, adenosine-5′-triphosphatase; F_1, pig heart mitochondrial F_1-ATPase; Tris, tris(hydroxymethyl)aminomethane; EDTA, ethylenediaminetetraacetic acid; BSA, bovine serum albumin; SDS, sodium dodecyl sulfate; TEG buffer, 30 mM Tris-HCl, pH 8 or 6.7, 1.2 mM EDTA, and 20% glycerol (v/v).

0006-2960/86/0425-2854$01.50/0

was estimated by the procedure of Lowry (Lowry et al., 1951) with BSA as the standard.

Electric Birefringence Measurements. The birefringence apparatus used in this study is described in detail elsewhere (Bernengo et al., 1973; Marion et al., 1984). To summarize briefly, the light source was a stable and noise-free He–Ne laser (Spectraphysics Model 120) with an emission wavelength of 632.8 nm, polarized at 45° with respect to the laser base. The Kerr cell has a 5-cm path length, and the electrode spacing was 0.2 cm. The cell could be filled with 0.85 mL of solution. All the measurements were made at room temperature. The pulse generator produced voltages ranging from 400 to 2000 V. The pulse duration could be varied from 10 μs to 0.1 ms with transition times of about 50 ns. After passing through a quarter-wave plate and an analyzer, the output from the birefringence cell was detected by a photodiode and optical amplifier. Birefringence signals delivered were displayed on an oscilloscope or stored in a transient recorder (Datalab DL 920) before analysis by computer. Rises and decays of birefringence signals were analyzed through a program based on a two-step adjustment fitting (Marion et al., 1984). The measurements described here have been repeated 5 times on different F_1-ATPase preparations.

Data Analysis. The fundamental principles of electric birefringence applied to macromolecular solutions have been described (Fredericq & Houssier, 1973), and only a few relations are presented in connection with the work carried out here.

The resulting steady-state birefringence (Δn_{eq}) is proportional to the square of the electric field (E^2) at low field strength. The specific Kerr constant (B) is defined

$$B = \Delta n_{eq}/C\lambda E^2 \tag{1}$$

where C is the solute concentration and λ the wavelength of the incident light.

The rise of birefringence [$\Delta R(t)$] depends on the value of E and the molecular electric properties. The birefringence decay [$\Delta D(t)$] depends only on the hydrodynamic properties of the solute. Dynamic birefringence equations are

$$\Delta D(t) = \Delta n(t)/\Delta n_{eq} = e^{-t/\tau} \tag{2}$$

$$\Delta R(t) = \Delta n(t)/\Delta n_{eq} = 1 - \frac{3r}{2(r+1)}e^{-t/3\tau} + \frac{r-2}{2(r+1)}e^{-t/\tau} \tag{3}$$

where $\Delta D(t)$ and $\Delta R(t)$ are normalized birefringences [$\Delta n(t)/\Delta n_{eq}$]. τ is the orientational relaxation time which is related to the rotational diffusion constant θ by $\tau = 1/6\theta$. In these equations, r characterizes the electric properties and orientation mechanism of the particles:

$$r = \mu^2/\Delta\alpha^E kT \tag{4}$$

where μ is the permanent dipole moment, $\Delta\alpha^E$ the electrical polarizability anisotropy, and kT the Boltzmann energy term.

Hydrodynamic Calculations. The rotational (θ) and translational (D) diffusion coefficients of particles with cylindrical symmetry are related to the dimensions of revolution ellipsoids through the general Perrin equation (Perrin, 1934):

$$\theta = \frac{kT}{8\pi\eta a^3 p^2} r(p) \tag{5}$$

$$D = \frac{kT}{6\pi\eta a p^{2/3}} t(p) \tag{6}$$

where η is the solvent viscosity and $r(p)$ a function of the axial ratio ($p = b/a$). The lengths of the axis of revolution and any perpendicular symmetry axis are $2a$ and $2b$, respectively. For different particle shapes, the forms of $r(p)$ are the following (only rotations of the longest axis have been considered):

$$r(p) = \frac{3p^2}{2(1-p^4)}\left[\frac{2-p^2}{\sqrt{1-p^2}}\ln\left(\frac{1+\sqrt{1-p^2}}{p}\right) - 1\right] \tag{7}$$

for a prolate ellipsoid ($a > b$, $p < 1$) and

$$r(p) = \frac{3p^2}{2(1-p^4)}\left[\frac{2-p^2}{\sqrt{p^2-1}}\operatorname{arctg}\left(\sqrt{p^2-1}\right) - 1\right] \tag{8}$$

for an oblate ellipsoid ($a < b$, $p > 1$). Similar equations are reported for translation and function $t(p)$ (Perrin, 1934).

According to a classical technique of hydrodynamic analysis (Daune et al., 1962; Bernengo et al., 1981), it is possible to combine D and θ values to get the axial ratio p and the main axis a, leading to the transcendental relation:

$$t^3(p)r^{-1}(p) = 27\left(\frac{\pi\eta}{kT}\right)^2\frac{D^3}{\theta} \tag{9}$$

Results

The electric birefringence of F_1-ATPase solution in 30 mM Tris-HCl, pH 8 or 6.7, 1.2 mM EDTA, and 20% glycerol (TEG buffer) was measured at various enzyme concentrations (ranging from 0.2 to 1 mg/mL). Measurements were performed at room temperature. Typical oscillograms of the birefringence of TEG buffer and of F_1 solution are shown in Figure 1. Because of the low degree of orientation attainable with the protein, high fields must be applied, ranging from 5000 to 10000 V/cm. Therefore, the solvent exhibits a positive birefringence (Figure 1c) that cannot be ignored, and then it must be subtracted from the signal obtained in birefringence of the enzyme solution.

Despite the relatively high electric fields used to orient the F_1 particles (5–10 kV/cm), no significant rise of temperature occurs during the pulse because of the very short orienting pulses applied, on the order of 20 μs. Besides, no changes in the electrooptical parameters are observed after the application of repeated pulses. On the other hand, ATPase activity is assayed before and after electric pulses. Under our experimental conditions, the activity remains constant (65 ± 4 μmol of ATP hydrolyzed min^{-1} mg^{-1}), showing that no denaturation is observed in the course of these measurements. The reproducibility of electrooptical measurements on different protein preparations is found to be very good, and the use of the solid-state photodetector to improve the signal to noise ratios allows a good accuracy on birefringence and relaxation time determinations. Parameters given below are averaged values of 25–30 measurements.

The birefringence of F_1-ATPase is clearly negative (Figure 1d). On application of a square electric pulse, the signal rises and practically reaches the steady state. The signal finally decays to the base line after removal of the field. A fast positive contribution to the birefringence is observed immediately after application of the field. It is due to the birefringence of the solvent which appears much more rapidly than that of the protein. This participation is revealed by the slow establishment of the steady state. The disymmetry of rise and decay curves clearly indicates a strong contribution of a permanent dipole moment to the orientation mechanism.

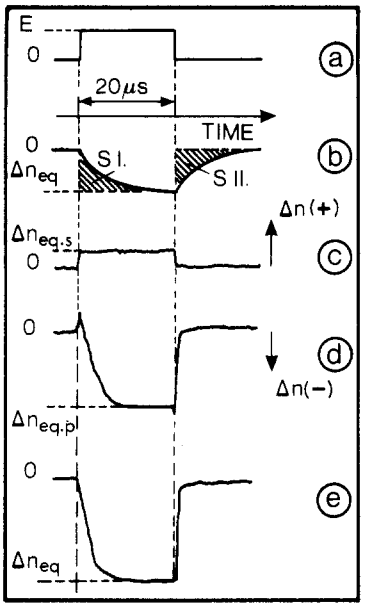

FIGURE 1: Electric birefringence of pig heart mitochondrial F_1-ATPase. (a) Electrical rectangular pulse with transition times of 50 ns. (b) Schematic illustration of a birefringence signal. The ratio of areas under the rise curve (SI) and decay curve (SII) can be related to the polarization mechanism. SI/SII reaches a maximum value of 4 when $r \rightarrow \infty$ (eq 4), i.e., for pure permanent moment, and it is equal to 1 when $r = 0$, i.e., for pure induced polarization. (c) Typical birefringence tracing obtained for TEG buffer (30 mM Tris-HCl, pH 6.7, 1.2 mM EDTA, and 20% glycerol). The field applied was 7.5 kV/cm. (d) Typical birefringence signal observed for F_1-ATPase in TEG buffer. The protein concentration was 1 mg/mL. (e) Actual birefringence of F_1-ATPase determined by subtracting the birefringence of the solvent (c) from that of the protein (d).

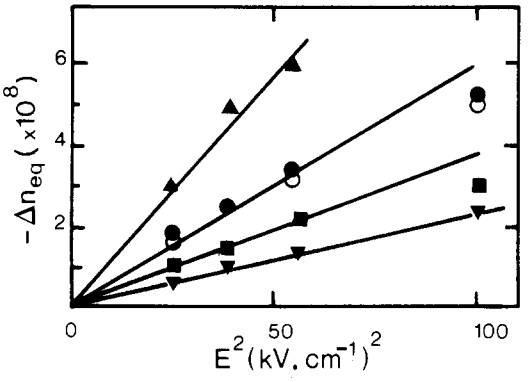

FIGURE 2: Steady-state birefringence of F_1-ATPase as a function of electric field. The protein concentration was 1 (▲), 0.6 (●, ○), 0.35 (■), and 0.23 mg/mL (▼). The pH of TEG buffer was 6.7 (▲, ●, ■, ▼) or 8.0 (○).

Great care has been taken to apply pulses long enough to reach steady-state birefringence, $\Delta n_{eq,p}$, before cutting off the electric field. Therefore, we are sure that the birefringence of F_1 can be calculated as $|\Delta n_{eq}| = |\Delta n_{eq,p}| + |\Delta n_{eq,s}|$ (Figure 1e). The pulse widths ranged from 15 to 60 μs, depending on the concentration and the amplitude of the applied field. The field dependence of the electric birefringence of F_1 at various protein concentrations is shown in Figure 2. The Kerr law (Δn_{eq} vs. E^2) is followed over the entire applied field range. The specific Kerr constant (calculated according to eq 1 from the slopes of the lines) is -1.5×10^{-3} esu cgs for the F_1-ATPase.

The steady-state birefringence is plotted in Figure 3 vs. concentration for F_1-ATPase in TEG buffer at several applied fields. Linear curves are obtained, showing that no molecular interaction leading to a decrease in polarizability or saturation can be detected in the concentration range studied.

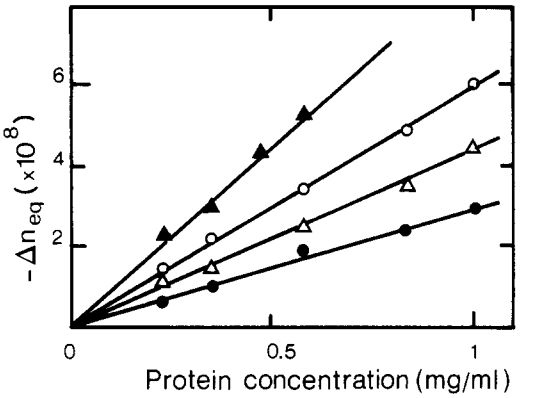

FIGURE 3: Concentration dependence of electric birefringence of F_1-ATPase. The electric fields applied were 10 (▲), 7.5 (○), 6.25 (▲), and 5 kV/cm (●). The pH of TEG buffer was 6.7.

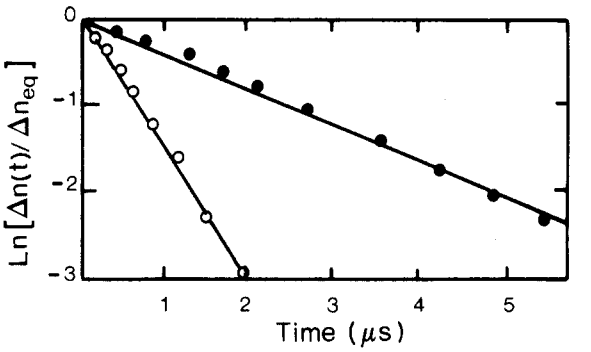

FIGURE 4: Analysis of dynamic birefringence of F_1-ATPase. Semilogarithmic plots of the rise (●) and decay (○) of the birefringence signal determined as described in Figure 1e. The protein concentration was 1 mg/mL, and the field applied was 7.5 kV/cm.

As shown in Figure 2, the specific birefringence of F_1-ATPase is insensitive to pH variation in the range 6.7–8. We recall that pH 8 is the optimal pH for ATP hydrolysis (Pullman et al., 1960) and that pH 6.7 is the pH necessary for the binding of P_i (Penefsky, 1977) or IF_1 (Pullman & Monroy, 1963).

Within the limits of experimental accuracy, birefringence decay curves have always been correctly fitted with a single-exponential decay. Figure 4 gives an example of the decay obtained.

The relaxation time was found to be concentration and field independent. The incubation of F_1-ATPase at pH 8 or 6.7 does not affect the value of τ.

The relaxation time was about 0.65 μs with a confidence interval given to 0.05-μs standard deviation. The remaining birefringence can be measured down to 5% of the steady-state value.

Consideration of the rise of anisotropy after the application of the field yields interesting information about the orientation mechanism of F_1-ATPase. Figure 1e shows the theoretical birefringence signal of the enzyme obtained by subtracting the effect of solvent (Figure 1c) from the experimental F_1 signal (Figure 1d). The predominance of a permanent dipole moment is obvious from the comparison of buildup and decay curves. We recall that at the field strength where the Kerr law is obeyed, the ratio of the areas SI and SII (Figure 1b) allows calculation of the ratio r of the contribution of the permanent dipole moment to that of the electrical anisotropy (eq 4). From our experiments made at different F_1 concentrations, we calculated an SI/SII ratio of about 3.6, very close to the maximum value of 4 observed when $r \rightarrow \infty$, i.e., for a pure permanent moment (Fredericq & Houssier, 1973).

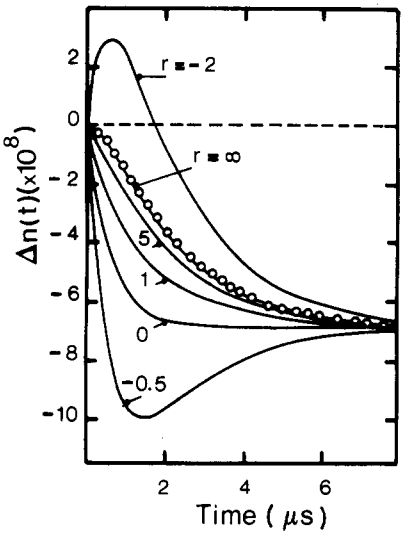

FIGURE 5: Analysis of the orientation mechanism of F_1-ATPase. Comparison of the experimental rise curve of birefringence (O) with the theoretical curves calculated from eq 3 by assuming a relaxation time of 0.65 μs.

The analysis of the rise curve is shown in Figure 4. The orientation time can be estimated to about 2.5–3 μs, and no dependence on field strength, enzyme concentration, and pH of TEG buffer was found.

To verify the existence of a strong permanent moment, theoretical curves of the rise of birefringence can be established (eq 3). Figure 5 shows curves obtained for different values of r and assuming for τ the value deduced from the decay (0.65 μs). Comparison with the actual curve (due to F_1 alone) clearly indicates that the best fit is reached for a value of r very close to infinity.

Discussion

We have described here an electric birefringence study of mitochondrial F_1-ATPase in solution. It should be mentioned at the outset that measurements were performed in buffers containing 20% glycerol in order to maintain both integrity and activity of the enzyme (Penin et al., 1979). Moreover, the presence of glycerol, by increasing the viscosity, makes the measurements of birefringence and relaxation times possible even with the low degree of orientation attainable with the protein.

What is very surprising is that F_1-ATPase exhibits a small but reproducible and significant negative birefringence. As far as we are aware, there are only two reports in the literature of proteins showing a negative electric birefringence: filaments of F-actin (Kobayasi et al., 1964) and soluble aggregates of paramyosin occurring at pH 6–7 (Krause & Delaney, 1977). The F_1-ATPase molecule has a smaller intrinsic Kerr constant than proteins previously studied in our laboratory, for example, spectrin (Roux & Cassoly, 1982) and connective tissue proteins (Bernengo et al., 1974, 1978, 1979). Repeated measurements showed that neither the specific birefringence nor the relaxation time is affected by protein concentration, pulse length, or the pH of the TEG buffer.

The decay curve of the birefringence always consists of only one component, down to 3–5% of the initial steady-state birefringence. Therefore, we are confident that no significant flexibility or reorientation occurs. We can also conclude that under our experimental conditions, there is no aggregation phenomenon and that the field-independent relaxation time observed (0.65 μs) corresponds to the orientation of the whole F_1-ATPase particle. This time allowed us to determine a rotational diffusion coefficient for pig heart mitochondrial F_1-ATPase of 2.55×10^5 s^{-1}. However, even in this simple case where a single rotary relaxation time is observed, a model has to be assumed to estimate the molecular dimensions. Although F_1 was first visualized as spherical particles of about 90-Å diameter (Kagawa & Racker, 1966; Howell & Moudrianakis, 1967; Munoz et al., 1968; Catterall & Pedersen, 1974; Garber & Steponkus, 1974; Yamato et al., 1978), it now appears that the F_1-ATPase is an oblate ellipsoid (Süss et al., 1978; Paradies & Schmidt, 1979; Satre & Zaccai, 1979; Amzel et al., 1982; Wagner & Junge, 1982; Ackey et al., 1983; Tiedge et al., 1983; Wagner et al., 1985). Therefore, the complete hydrodynamical characterization of such a particle is possible only if at least a second parameter is available. We can use the translational diffusion constant D, estimated from previous work on pig heart mitochondrial F_1-ATPase. Di Pietro et al. (1975) have calculated a sedimentation coefficient ($s^0_{20,w}$) of 12.4 S, and by assuming a molecular weight of 371 000 (Walker et al., 1985), for the enzyme we determined a value $D^0_{20,w} = 3.10 \times 10^{-7}$ cm^2 s^{-1}. According to a well-known hydrodynamical analysis based on Perrin formulas (Daune et al., 1962; Bernengo et al., 1981), it is possible to combine θ and D values to get the axial ratio $p = b/a$ and the main axis of an equivalent oblate ellipsoid (eq 9). However, to eliminate the influence of buffer viscosity, the measured θ must be corrected to standard conditions. With the corrected value of 4.4×10^5 s^{-1}, we obtain $p = 2.5$ and $L = 170$ Å, i.e., overall dimensions of 170 × 170 × 70 Å, very close to the dimensions estimated by Süss et al. (1978) and by Wagner (Wagner & Junge, 1982; Wagner et al., 1985). In an X-ray study, Süss et al. (1978) have calculated dimensions for an oblate ellipsoid of 168 × 168 × 84 Å. Rotational diffusion measurements suggested similar overall dimensions for the enzyme, 180 × 180 × 70 Å (Wagner & Junge, 1982), and recent measurements using time-resolved laser spectroscopy gave 170 × 170 × 85 Å (Wagner et al., 1985). These results are strikingly different from the smaller volumes obtained by X-ray and neutron scattering (Paradies & Schmidt, 1979; Satre & Zaccai, 1979). The discrepancy likely arises from the hydration brought about by glycerol, which may change the composition of the solvent around the molecule, affecting its diffusion properties (Fredericq & Houssier, 1973). Our work suggested a molecular volume of 1060 nm^3 while the dried volume was found to be 460 nm^3 by assuming an anhydrous specific volume of 0.74 cm^3/g (Penefsky & Warner, 1965). The degree of hydration can be estimated to 0.94 g of water/g of protein. This high solvation is very close to that of 1 g/g calculated for thermophilic bacterial F_1 (Paradies & Kagawa, 1982).

The birefringence of F_1 is negative; i.e., the molecule is oriented with the long axis perpendicular to the direction of the field. Analysis of the rise curves of birefringence has allowed us to discriminate easily between the contributions of permanent dipole and induced polarizability to the orientation mechanism. Therefore, the orientation of ATPase is caused by a permanent moment perpendicular to the long axis of the particle. These particular electric properties of F_1 could be explained by the topographical organization of its five subunits, α, β, γ, δ, and ϵ. For mitochondrial ATPase, the stoichiometry $\alpha_3\beta_3\gamma\delta\epsilon$ is now widely accepted. By X-ray diffraction, the F_1 molecule appears to be formed by two equivalent halves, each formed by three regions of approximately equal size (Amzel et al., 1982). These regions form a distorted hexagonal or octahedral arrangement with a central hole. One attractive possibility is that in the side by side association of subunits, the presence of only one protein with

its long axis perpendicular to the long axis of the whole F_1 particle could be sufficient to explain the negative birefringence of F_1. Indeed, if this subunit protein is oriented by a permanent moment, its association with the other subunits into F_1-ATPase results in the appearance of a dipole perpendicular to the long axis of the whole particle. Further direct work on isolated subunits will be needed to identify the protein(s) involved.

ACKNOWLEDGMENTS

We thank Professor D. C. Gautheron and Dr. C. Godinot for initiation of the work and stimulating discussions and F. Penin for his kind cooperation in pig heart mitochondrial F_1-ATPase preparation, Z. Hernaus for the drawings, and B. Duclot for typing the manuscript.

Registry No. ATPase, 9000-83-3.

REFERENCES

Ackey, C. W., Spitzberg, V., & Edelstein, S. J. (1983) *J. Biol. Chem. 258*, 3222–3229.

Amzel, L. M., & Pedersen, P. L. (1983) *Annu. Rev. Biochem. 52*, 801–824.

Amzel, L. M., McKinney, M., Narayanan, P., & Pedersen, P. L. (1982) *Proc. Natl. Acad. Sci. U.S.A. 79*, 5852–5856.

Bernengo, J. C. (1981) in *Molecular Electro-Optics* (Krause, S., Ed.) pp 341–362, Plenum Press, New York.

Bernengo, J. C., Roux, B., & Hanss, M. (1973) *Rev. Sci. Instrum. 44*, 1083–1087.

Bernengo, J. C., Roux, B., & Herbage, D. (1974) *Biopolymers 13*, 641–647.

Bernengo, J. C., Herbage, D., Marion, C., & Roux, B. (1978) *Biochim. Biophys. Acta 532*, 305–314.

Bernengo, J. C., Roux, B., & Herbage, D. (1979) in *Electro-Optics and Dielectrics of Macromolecules* (Jennings, B., Ed.) pp 219–230, Plenum Press, New York.

Bernengo, J. C., Bezot, P., Bezot, C., Roux, B., & Marion, C. (1981) *Ber. Bunsen-Ges. Phys. Chem. 85*, 657–661.

Catterall, W. A., & Pedersen, P. L. (1974) *Biochem. Soc. Spec. Publ. 4*, 63–88.

Daune, M., Freund, L., & Spach, G. (1962) *J. Chim. Phys. Phys.-Chim. Biol. 59*, 485–491.

Delêage, G., Penin, F., Godinot, C., & Gautheron, D. C. (1983) *Biochim. Biophys. Acta 725*, 464–471.

Di Pietro, A., Godinot, C., Bouillant, M. L., & Gautheron, D. C. (1975) *Biochimie 57*, 959–967.

Di Pietro, A., Penin, F., Godinot, C., & Gautheron, D. C. (1980) *Biochemistry 19*, 5671–5678.

Fillingame, R. H. (1980) *Annu. Rev. Biochem. 49*, 1079–1113.

Fredericq, E., & Houssier, C. (1973) in *Electric Dichroism and Birefringence* (Harrington, W., & Peacoke, A. R., Eds.) Clarendon Press, Oxford.

Garber, M. P., & Steponkus, P. I. (1974) *J. Cell Biol. 63*, 24–34.

Godinot, C., Vial, C., Font, B., & Gautheron, D. C. (1969) *Eur. J. Biochem. 8*, 385–394.

Godinot, C., Di Pietro, A., & Gautheron, D. C. (1975) *FEBS Lett. 60*, 250–255.

Howell, S. H., & Moudrianakis, F. M. (1967) *Proc. Natl. Acad. Sci. U.S.A. 58*, 1261–1268.

Kagawa, Y., & Racker, E. (1966) *J. Biol. Chem. 241*, 2475–2482.

Kobayasi, S., Asai, H., & Oosawa, F. (1964) *Biochim. Biophys. Acta 88*, 528–540.

Krause, S., & Delaney, D. E. (1977) *Biopolymers 16*, 1167–1181.

Laemmli, H. K. (1970) *Nature (London) 222*, 680–685.

Lowry, O. H., Rosebrough, N. J., Farr, A. L., & Randall, R. J. (1951) *J. Biol. Chem. 193*, 265–275.

Marion, C. (1984) *J. Biomol. Struct. Dyn. 2*, 303–317.

Marion, C., & Roux, B. (1978) *Nucleic Acids Res. 5*, 4431–4449.

Marion, C., Roux, B., & Bernengo, J. C. (1984) *Makromol. Chem. 185*, 1647–1664.

Marion, C., Roche, J., Roux, B., & Gorka, C. (1985a) *Biochemistry 24*, 6328–6335.

Marion, C., Martinage, A., Tirard, A., Roux, B., Daune, M., & Mazen, A. (1985b) *J. Mol. Biol. 186*, 367–379.

Mitchell, P. (1961) *Nature (London) 191*, 144–148.

Munoz, E., Freer, J. H., Ellar, D. J., & Salton, M. R. (1968) *Biochim. Biophys. Acta 150*, 531–533.

Paradies, H. H., & Schmidt, U. D. (1979) *J. Biol. Chem. 254*, 5257–5263.

Paradies, H. H., & Kagawa, Y. (1982) *FEBS Lett. 137*, 25–29.

Paradies, H. H., Zimmerman, J., & Schmidt, U. D. (1978) *J. Biol. Chem. 253*, 8972–8979.

Penefsky, H. S. (1977) *J. Biol. Chem. 252*, 2891–2899.

Penefsky, H. S., & Warner, R. C. (1965) *J. Biol. Chem. 240*, 4694–4702.

Penin, F., Godinot, C., & Gautheron, D. C. (1979) *Biochim. Biophys. Acta 548*, 63–71.

Perrin, F. (1934) *J. Phys. Radium 5*, 497–511.

Pullman, M. E., & Monroy, G. C. (1963) *J. Biol. Chem. 238*, 3762–3769.

Pullman, M. E., Penefsky, H. S., Datta, A., & Racker, E. (1960) *J. Biol. Chem. 235*, 3322–3329.

Roux, B., & Cassoly, R. (1982) *Biophys. Chem. 16*, 193–198.

Roux, B., Felloux, G., & Godinot, C. (1984) *Biochemistry 23*, 534–537.

Satre, M., & Zaccai, G. (1979) *FEBS Lett. 102*, 244–248.

Süss, K. H., Damaschun, H., Damaschun, G., & Zirwer, D. (1978) *FEBS Lett. 87*, 265–268.

Tiedge, H., Schäfer, G., & Mayer, F. (1983) *Eur. J. Biochem. 132*, 37–45.

Vignais, P. V., & Satre, M. (1984) *Mol. Cell. Biochem. 60*, 33–70.

Wagner, R., & Junge, W. (1982) *Biochemistry 21*, 1890–1899.

Wagner, R., Engelbrecht, S., & Andreo, C. S. (1985) *Eur. J. Biochem. 147*, 163–170.

Walker, J. E., Fearnley, I. M., Gay, N. J., Gibson, B. W., Northrop, F. D., Powell, S. J., Runswick, M. J., Saraste, M., & Tybulewicz, V. L. J. (1985) *J. Mol. Biol. 184*, 677–701.

Yamato, I., Futai, M., Anraku, Y., & Nonomura, Y. (1978) *J. Biochem. (Tokyo) 83*, 117–128.

Yoshioka, K. J. (1978) *Electro-Opt. Ser. 2*, 601–644.